Colloid Polym Sci (2006) 285:351–358
DOI 10.1007/s00396-006-1578-4

ORIGINAL CONTRIBUTION

Thermo-sensitive colloidal crystals of silica spheres in the presence of large spheres with poly (*N*-isopropyl acrylamide) shells

Tsuneo Okubo · Taro Mizutani · Junichi Okamoto · Keisuke Kimura · Akira Tsuchida · Klaus Tauer · Victor Khrenov · Haruma Kawaguchi · Sakiko Tsuji

Received: 20 April 2006 / Accepted: 27 July 2006 / Published online: 6 October 2006

Abstract Thermo-sensitive colloidal crystals are prepared simply by mixing colloidal silica spheres and large thermo-sensitive gel spheres. The thermo-reversible change in the lattice spacing of colloidal crystals of monodisperse silica spheres (CS82, 103 nm in diameter) depends on the size of the admixed temperature-sensitive gel spheres. For spheres with sizes less and greater than that of the silica spheres, the lattice spacing upon temperature increase above the lower critical solution temperature of poly(*N*-isopropyl acrylamide) decreases (cf. Okubo et al. Langmuir 18:6783, 2002) and increases, respectively. A mechanism, which is able to explain these experimental findings, is proposed. Moreover, crystal growth rates and the rigidities of the thermo-sensitive colloidal crystals are studied.

T. Okubo (✉)
Institute for Colloidal Organization,
Hatoyama 3-1-112,
Uji, Kyoto 611-0012, Japan
e-mail: okubotsu@ybb.ne.jp

T. Okubo
Cooperative Research Center, Yamagata University,
Yonezawa 992-8510, Japan

T. Mizutani · J. Okamoto · K. Kimura · A. Tsuchida
Department of Applied Chemistry, Gifu University,
Gifu 501-1193, Japan

K. Tauer · V. Khrenov
Max Planck Institute of Colloids and Interfaces,
Golm D-14424 Potsdam, Germany

H. Kawaguchi · S. Tsuji
Graduate School of Science and Technology, Keio University,
Hiyoshi Yokohama 223-8522, Japan

Keywords Thermo-sensitive colloidal crystal · Colloidal silica sphere · Poly(*N*-isopropyl acrylamide) · Lattice spacing · Crystal growth rate · Rigidity

Introduction

Recently, keen attention was paid to colloidal crystals, i.e., crystal-like distribution of colloidal particles in suspensions of aqueous and organic solvents. In general, most colloidal particles in aqueous suspension get negative charges on their surfaces by two mechanisms; one is the dissociation of ionizable groups and the other is the preferential adsorption of ions from suspension. These ionic groups leave their counterions, and the excess charges accumulate near the surface forming an electrical double layer. When the suspension is exhaustively deionized with the mixed beds of the ion-exchange resins, the electrical double layers expand and the particles arrange regularly. In other words, an essential interaction for colloidal crystallization is the interparticle electrostatic *repulsion* accompanied with the extended electrical double layers around the particles [1–19]. It should be mentioned further that most research on colloidal crystals were for the structures formed in the closed and equilibrium states. However, some researchers including our group have studied the crystalline structures formed in the course of energy dissipation and non-equilibrium state [20–27]. Recently, the author's group clarified the cationic-charged colloidal crystals being formed, though the spheres were not so stable chemically [28]. Furthermore, core-shell type spheres formed colloidal crystal structures in deionized aqueous media [29]. Electro-optic effects of the immobilized colloidal crystals were also studied [30].

Several types of thermo-sensitive spheres including the core-shell type were reported hitherto [31–34]. Recently, the thermo-sensitive colloidal crystals of *N*-isopropylacrylamide (NIPAAm) derivative polymer hydrogel were prepared [35–37]. The authors reported that the thermo-sensitive colloidal crystals were formed simply by mixing colloidal silica spheres with smaller size of NIPAAm gel spheres in aqueous suspension state [38]. Present work further investigates the preparation of thermo-sensitive colloidal crystals by mixing colloidal silica spheres with larger latex spheres containing poly-NIPAM (PNIPAM) shells. It is interesting to note that the results show that the change of the lattice spacing upon temperature increase depends on the size ratio between the silica and latex spheres.

Experimental

Materials

Monodispersed colloidal silica spheres (CS82, 103 nm± 13.2 nm in diameter) were donated by Catalyst and Chemicals (Tokyo). The surface charge density of strongly acidic charges of CS82 spheres was determined to be 0.38 μC/cm^2 by conductometric titration with a Horiba Model DS-14 conductivity meter (Kyoto). Stock suspension was deionized with ion-exchange resins (BioRad, AG501-X8(D), 20–50 mesh, Richmond, CA) for more than 10 years. The sample suspensions prepared in the cell with the ion-exchange resins coexisted at least 1 week before the measurements.

Thermo-sensitive TG and SVN gel spheres were prepared in Tauer's and Kawaguchi's laboratories, respectively. The TG spheres are triblock copolymer spheres composed of poly(ethylene glycol)-*b*-PNIPAM-*b*-poly (methyl methacrylate) and were prepared as described in a previous paper [39]. The SVN sphere consists of a styrene-vinylbenzyl chloride copolymer as core surrounded by a hairy layer of poly(*N*-isopropylacrylamide), PNIPAM chains. Details of the preparation of the sample spheres were described in a previous paper [40]. Change in the hydrodynamic diameters in dependence on the temperature was determined with dynamic light scattering and is shown for both types of spheres in Fig. 1.

The water used for the sample preparation was purified by a Milli-Q reagent grade system (Milli-RO5 plus and Milli-Q plus, Millipore, Bedford, MA).

Dynamic light scattering (DLS) measurements

DLS measurements were made with a DLS spectrophotometer (DLS-7000, Otsuka Electronics, Hirakata, Osaka) in a cylindrical vat containing silicone oil. A 5-ml sample suspension was prepared in a Pyrex tube cell (12-mm outside diameter and 130-mm long). Data analysis was made with the cumulant analysis method.

Reflection spectroscopy

The reflection spectra of the suspension at various temperatures, at an incident angle of 90° through the quartz glass of the bath, the water in the bath and the quartz glass of the optical cell were recorded on a multi-channel photo detector (MCPD-7000G3, Otsuka Electronics) connected to a Y-type optical fiber cable. A test tube (8-ml, 10 mm in inner diameter and 100 mm high, NN-13, Maruemu, Osaka) was set in the water bath of quartz glass. Temperature in the bath was controlled by the circulating water from a

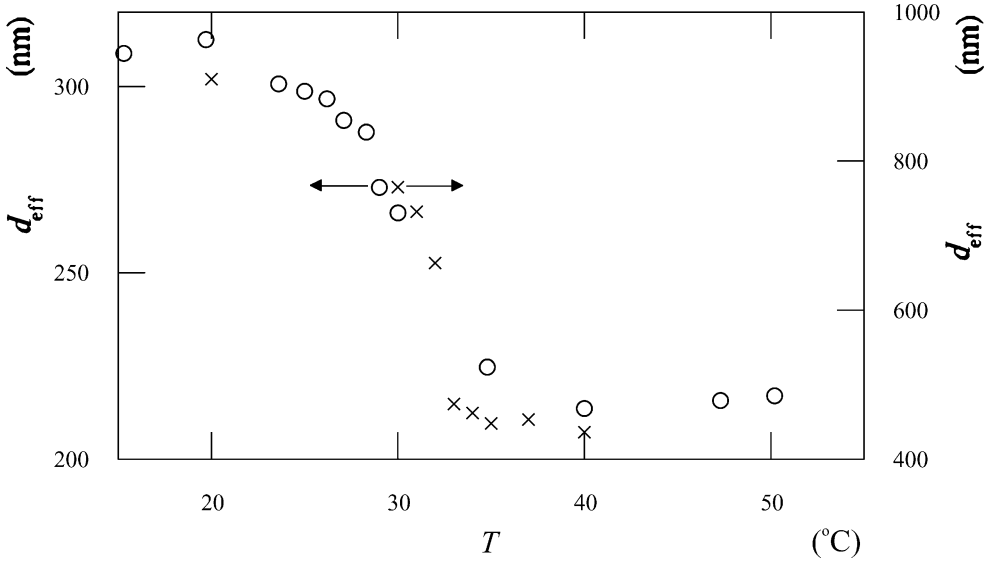

Fig. 1 Change in the effective diameter of TG and SVN gel spheres as a function of temperature. *Open circle*: TG, *open square*: SVN

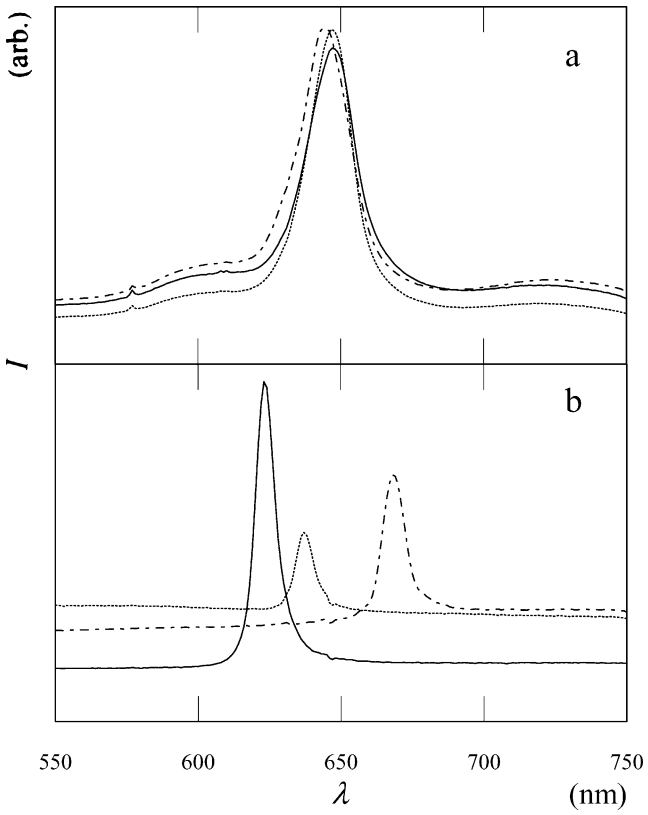

Fig. 2 Reflection spectra of CS82 suspensions (**a**) and the mixtures of CS82 and TG gel spheres (**b**) as a function of temperature. ϕ=0.032, (**a**) w=0 g/ml, (**b**) 0.02 g/ml, *solidcurve*: T=15 °C, *dottedcurve*: 35 °C, *dotted brokencurve*: 50 °C

thermostat (RTE-211, Neslab Instruments, Newington) and changed between 15 °C and 55 °C.

The crystal growth rate was measured from the sharpened peaks in the reflection spectra at different times after the sample suspensions were set to stand still in the bath. The rigidity of the crystal was determined from the reflection spectroscopy in the sedimentation equilibrium. The observation cell was the same as used for the reflection spectroscopy, and set in a test tube support. A sample suspension of 6 ml volume was introduced into the cell. About 0.5 ml of a mixed bed of ion-exchange resins [BioRad, AG501-X8(D)] was further added. Then, the cells were left to stand after mixing. The reflection spectra at various heights at an incident angle of 90° were recorded over a period of 2 months on a multi-channel photodetector.

Results and discussion

Temperature dependence of size of gel spheres

Figure 1 shows the change in the hydrodynamic diameter, d_{eff} of TG and SVN gel spheres as a function of suspension temperature, T. For both samples, the diameters decreased transitionally at ca. 35 °C when temperature increased. The diameters for TG and SVN spheres decreased from 310 nm at 25 °C to 215 nm at 50 °C, and from 970 nm at 15 °C to 479 nm at 55 °C, respectively, corresponding to a volume change by a factor of 3 and 8, respectively. The shrinkage is completely reversible when the temperature is decreased again.

Reflection spectroscopy of the suspension mixtures of CS82 and NIPAAm gel spheres

Typical examples of the reflection spectra of CS82 and TG gel mixtures are shown in Fig. 2. The reflection spectra of the pure CS82 colloidal crystals were quite insensitive to the suspension temperature as shown clearly in Fig. 2a. On the other hand, the peaks of the CS82 and TG mixtures

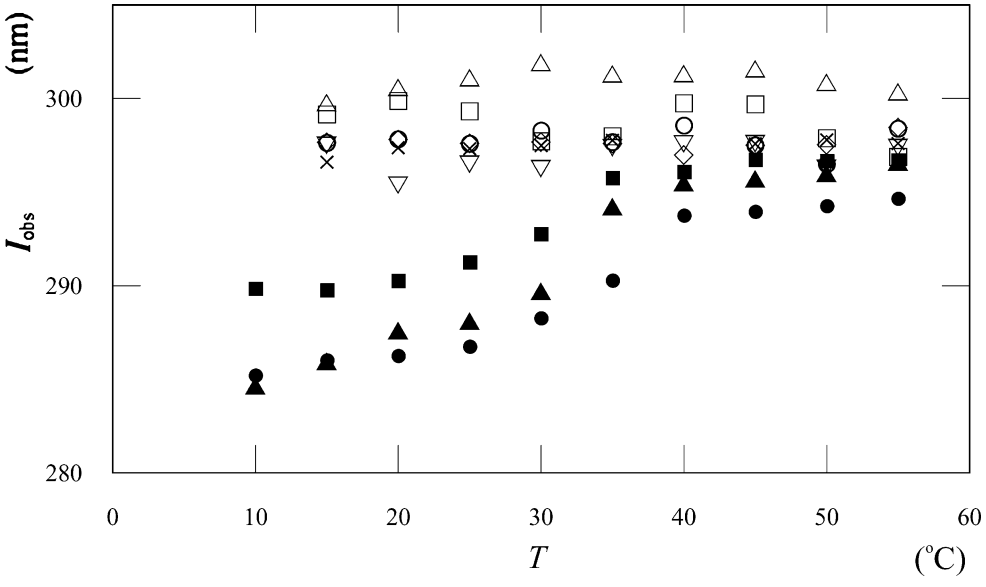

Fig. 3 Changes in the inter-sphere spacing (l_{obs}) of the mixtures of CS82 and TG gel spheres. ϕ=0.032, *open circle*: w=0 g/ml, cross: 0.0001, *open triangle*: 0.0003, *open square*: 0.001, *inverse open triangle*: 0.0025, *diamond*: 0.003, *solid circle*: 0.0083, *solid triangle*: 0.0167, *solid square*: 0.0200

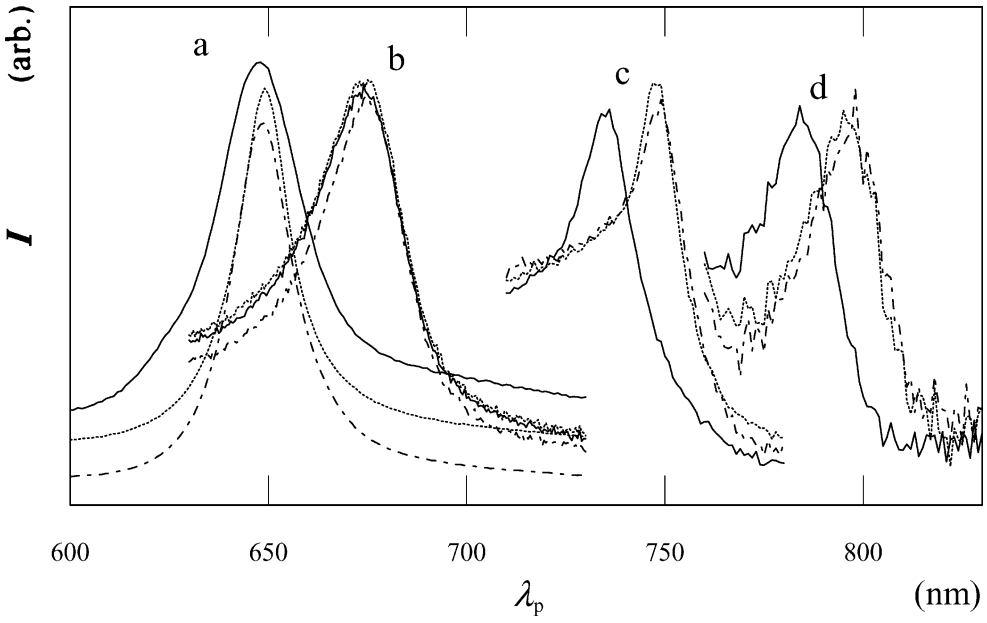

Fig. 4 Reflection spectra of the mixtures of CS82 and SVN spheres. ϕ=0.032, (**a**) w=0 g/ml, (**b**) 0.0042 g/ml, (**c**) 0.0083 g/ml, (**d**) 0.01 g/ml, *solid curve*: 15 °C, *dotted curve*: 35 °C, *dotted broken curve*: 55 °C

shifted transitionally when the temperature increased as shown in Fig. 2b. These changes in the peak wavelengths indicate clearly that the expansion and contraction of the crystal lattice at low and high temperatures, respectively, were obviously caused by the TG gel spheres.

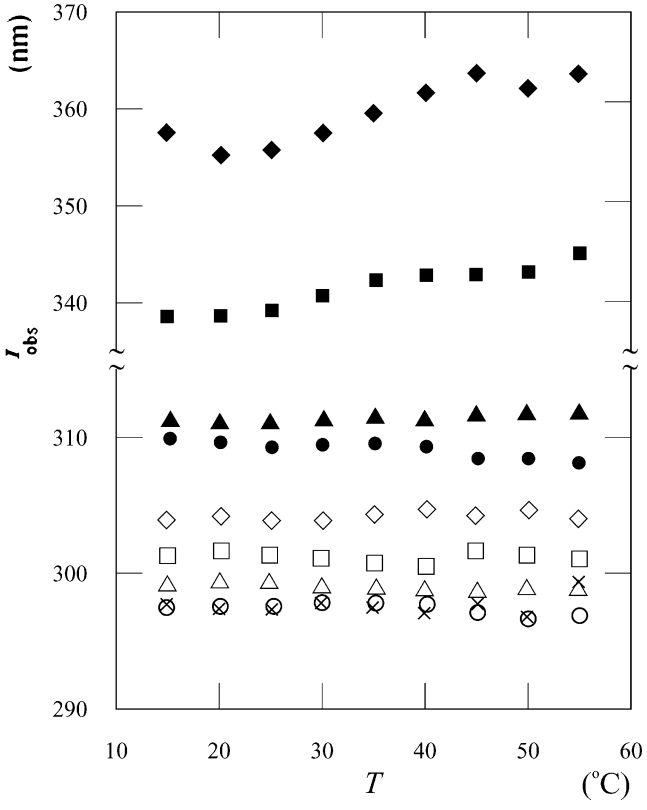

Fig. 5 Changes in the intersphere spacing (l_{obs}) of the mixtures of CS82 and SVN gel spheres. ϕ=0.032, *open circle*: w=0 g/ml, *cross*: 0.0001, *open triangle*: 0.0003, *open square*: 0.001, *open diamond*: 0.0025, *solid circle*: 0.003, *solid triangle*: 0.0042, *solid square*: 0.0083, *solid diamond*: 0.01

The lattice spacings, the nearest-neighbored intersphere distances, in face-centered cubic (*fcc*) and body-centered cubic (*bcc*) lattices ($l_{obs,f}$ and $l_{obs,b}$) are given by Eq. 1.

$$l_{obs,f} = l_{obs,b} = 0.6124\left(\lambda_p / n_s\right), \tag{1}$$

where λ_p denotes the wavelength of the primary reflection peak and n_s indicates the refractive index of the sample suspension. In this work, n_s was taken as 1.333 at 25 °C, which is the value of water because the measurements were made at rather low sphere and gel concentrations. From our experiences, the lattice structure of the colloidal crystals of silica spheres in the absence of the gel spheres is assumed to be *fcc* because the sphere concentration of 0.032 in volume fraction is high enough for the formation of *fcc* lattices. Much work has reported that the *fcc* lattices are more stable than *bcc* at high sphere concentrations [12]. The lattice spacing calculated for a simple cubic lattice, l_o, is given by Eq. 2.

$$l_o = 0.904 d_o \phi^{-1/3}, \tag{2}$$

where d_o and ϕ are the diameter in nm and the concentration of the colloidal silica spheres in volume fraction, respectively.

Figure 3 shows the l_{obs} of CS82 and TG mixtures as a function of suspension temperature and the content of TG. In the absence of gel spheres (w=0 g/ml), l_{obs} was quite insensitive to suspension temperature. l_{obs} and l_o values of 284 and 293 nm, respectively, agree satisfactorily. By the addition of gel spheres, l_{obs} increased and then decreased, though l_{obs} was insensitive to temperature, when the gel spheres concentrations were lower than 0.003 g/ml, as

clearly seen in the figure. It is surprising to note that by the addition of the gels at concentrations higher than w=0.0042, l_{obs} values increased transitionally as suspension temperature increased. The critical temperature of the transition was ca. 35 °C and coincided almost with that of the TG.

Figure 4 shows the reflection spectra of the mixtures of CS82 spheres and SVN gel spheres. The transitional peak shifts toward long wavelengths were observed clearly as the content of SVN increased. Figure 5 shows the l_{obs} values as a function of temperature for the CS82 and SVN mixtures. They increased again by the addition of SVN gel spheres, when the gel spheres concentration was lower than 0.0042 g/ml, l_{obs} was quite insensitive to suspension temperature. However, l_{obs} increased transitionally by the addition of SVN spheres at the concentrations higher than w=0.0083 g/ml as clearly seen in the figure.

It has to be noted that these temperature dependencies of l_{obs} in this work are opposite to those found previously for mixtures where the size of the gel spheres was less those of the silica spheres [38]. Obviously, the size ratio of the gel spheres against silica spheres is important for the thermo-sensitivity in our colloidal crystal systems.

Mechanism of the thermo-sensitive expansion and contraction in the crystal lattices

In our previous work [38], the intersphere spacings l_{obs} were quite insensitive to suspension temperature in the absence of gel spheres. In the presence of the small gel spheres, on the other hand, l_{obs} decreased transitionally at 35 °C when suspension temperature increased. In the presence of small gel spheres, the gel spheres locate between the neighboring silica spheres and bind weakly with the silica surfaces. Furthermore, the gel spheres are quite soft and vague in the outer boundary. Thus, the expansion and/or contraction of the gel spheres with temperature results in the expansion and/or contraction in the lattice spacing of the crystal structure of the silica spheres.

When the size of gel spheres is large in this work, the gels are not located between the neighboring silica spheres without breaking the crystal lattices. Then, it is highly plausible that most of the large gel spheres are segregated from the crystal regions of the silica spheres. A schematic picture of the thermo-sensitive colloidal crystals formed in the mixtures of CS82 spheres and TG gels is shown in Fig. 6. In this scheme, the expansion and/or contraction of the gel spheres with temperature results in the contraction and/or expansion of the lattice spacing in the crystal regions, when the sum of the gel and crystal regions are kept constant in the vessel.

The SVN gel spheres are composed of polystyrene core and PNIPAAm shell parts. The hairy layer is hydrophilic enough to invite silica spheres in it, and parts of silica spheres are highly plausible to be bound in the inner shell of PNIPAAm. This situation may result in the decrease of the silica spheres in the crystal regions, and then in the increase of the lattice spacing. It should be further mentioned here that the segregation effect of the gel regions from the crystal regions should be incomplete for the hairy and very soft nature of gel spheres especially for the big SVN gels.

Kinetic analyses of the thermo-sensitive colloidal crystallization

The size of the colloidal single crystals from the homogeneous nucleation, L, is estimated from the peak intensity (I) in the reflection spectra [41, 42],

$$I \cong N_{cryst} L^3 \cong L^3 \quad (3)$$

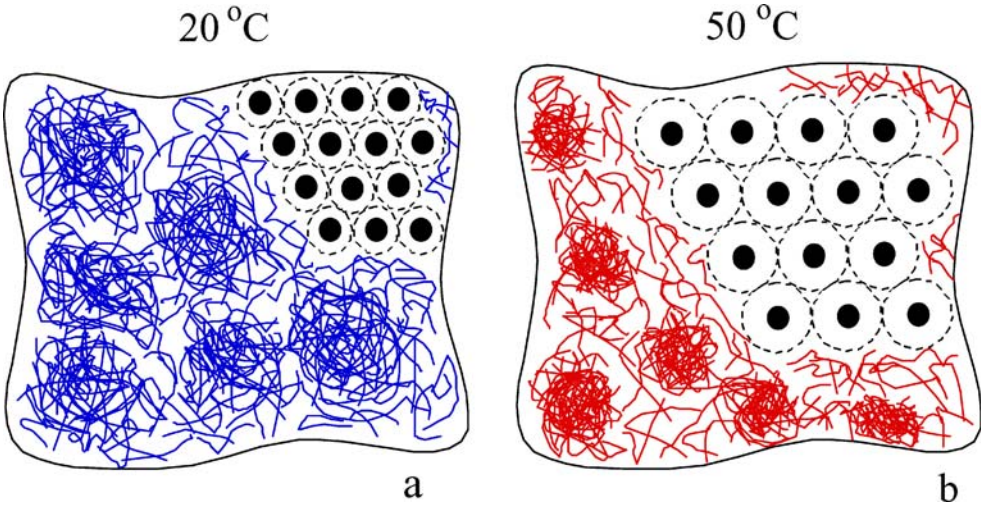

Fig. 6 Schematic representation of colloidal crystals of the mixtures of CS82 and TG gel spheres: (**a**) at 20 °C, and (**b**) at 50 °C

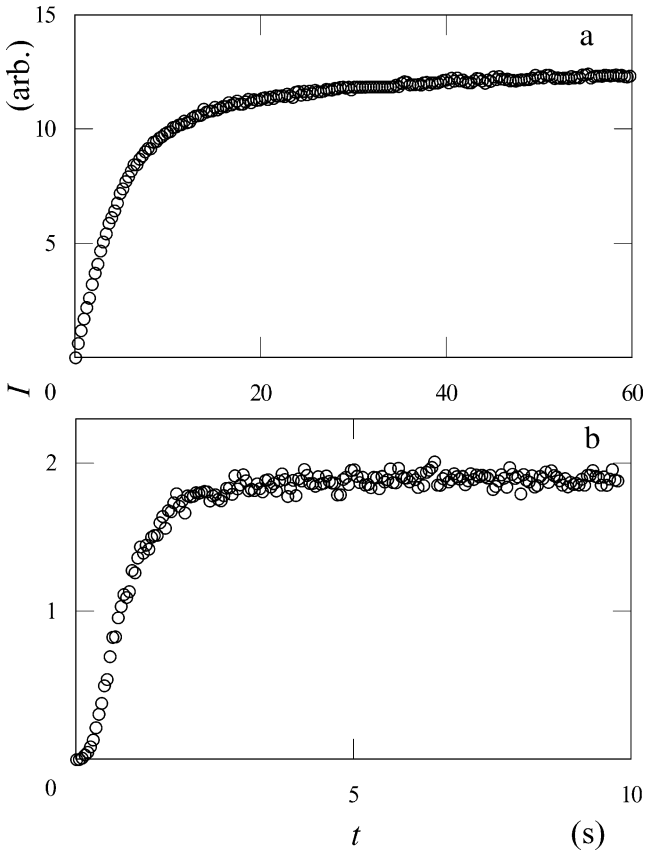

Fig. 7 Plots of the reflection peak intensity for the mixtures of CS82 and TG (**a**) and CS82 and SVN (**b**) spheres as a function of time at 25 °C. ϕ=0.032, *curve a*: w=0.003 g/ml, *curve b*: 0.0042

where N_{cryst} is the number of single crystals in the reflecting volume, which is directly proportional to the number concentration of crystals in the final stages of the crystallization process, being equal to the total number of nuclei formed in the whole course of crystallization.

Figure 7a and b shows the typical traces of the peak intensity for the mixtures of CS82+TG and CS82+SVN, respectively in the course of crystallization. The intensity increased with time and eventually reached a constant value. It should be noted here that the silica spheres concentration is rather high, 0.032 in volume fraction. Thus, the idea that the observed change in the peak intensity corresponds to the *secondary* crystallization step where the metastable and rather loose crystals, which formed in the first crystallization step, become stable and compact ones [42].

Figure 8 shows the apparent crystal growth rates k obtained from the initial slope in the peak intensity vs time curves. k decreased as w increased. This result clearly supports the idea that the much larger gel spheres disturb the secondary crystallization process mainly by the distortion of the crystal structure formed in the primary step.

Rigidity of the thermo-sensitive colloidal crystals

The peak wavelengths in the reflection spectra of CS82+TG and CS82+SVN mixtures changed very slowly and the sedimentation equilibrium state was achieved after 2 months that the suspensions were set. In the sedimentation equilibrium, Eq. 4 holds [43].

$$\lambda_p - \lambda_{p,m} = \left(\rho_{eff} g_o \lambda_{p,m} \phi_m / G\right)(h - h_m) \tag{4}$$

Here, $\lambda_{\mathrm{p,m}}$ and ϕ_m indicate the lattice spacing and the sphere concentration at the mid-plane of the cell, h_{m}, respectively. ϕ_m is, therefore, equal to the initial concentration of CS82 spheres. ρ_{eff} is the effective density given by the specific gravity of the spheres minus that of the solvent, and g_0 is the gravitational constant. h is the height from the bottom of the cell. G is Young's elastic modulus for the

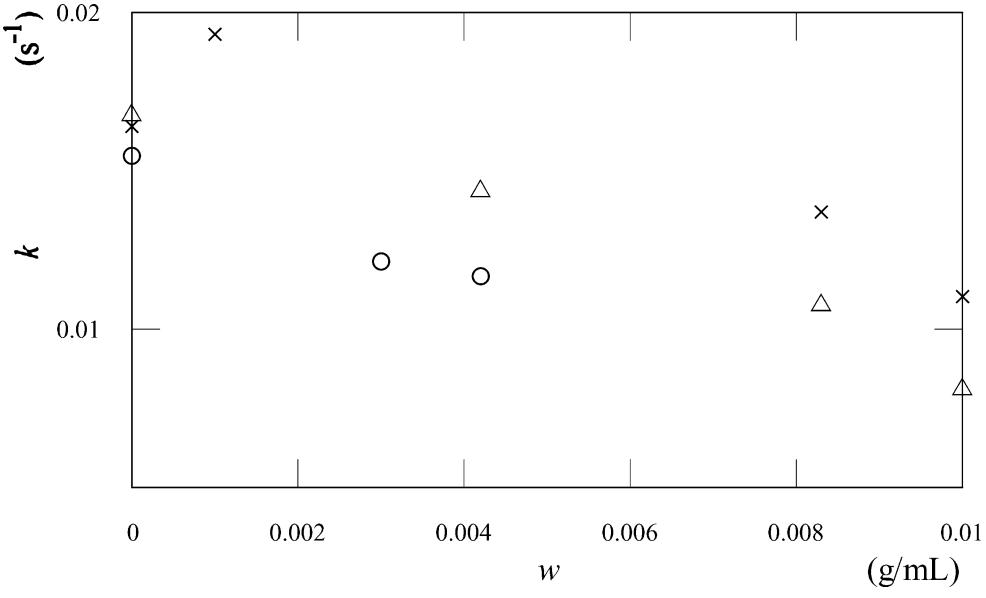

Fig. 8 Apparent crystallization rates for the mixtures of CS82+TG (*open circles*), CS82+SVN (*crosses*) and CS82+KG (*open triangles*) as a function of the gel concentration at 25 °C. ϕ=0.032

colloidal crystals, which is obtained from the slopes of λ_p vs h graphs. It should be mentioned here that the linearity between λ_p and h was satisfactory.

Table 1 compiles the elastic moduli, G, thus obtained. Here, N_p and N_g are the number densities of silica spheres and gel spheres, respectively. G values of CS82+TG and CS82+SVN kept constant around 260 Pa, and decreased, as gel concentration increased. It should be recalled that the G values of CS82+KG [38] increased slightly as w increased. The increase in rigidity by the addition of gels was explained by the increased contribution from the rigidity of the gel spheres themselves [38]. One of the main reasons for the decrease tendency of the G values with increasing w, on the other hand, is the distortion of the crystal structures by the addition of the gels. The authors believe that concentration dependencies in the rigidities of the mixtures are determined by two competing factors, i.e., increase in the inherent rigidity of the gels and decrease in the rigidity of the crystals by the distortion of the order in the silica crystals.

Generally speaking, the elastic modulus G of the colloidal crystal is written in terms of the magnitude of the thermal fluctuation, δ, of a sphere as [19, 44].

$$G \cong f/l \cong \left(k_B T / < \delta^2 > \right)/l \tag{5}$$

Here, f and l are the force constants between colloidal spheres and the nearest-neighbor intersphere distance in the colloidal crystals, δ is the thermal fluctuation of a sphere in the effective potential valley, k_B is the Boltzmann constant, and T is the suspension temperature. Introducing a non-dimensional parameter g for $<\delta 2>/l$, the modulus is obtained as a linear function of the number density of spheres, N,

$$G \cong N k_B T / g^2 \tag{6}$$

When g is unity, Eq. 6 gives the elastic modulus of an ideal liquid having the same sphere concentration. Lindemann's law of crystal melting tells us that $g<0.1$ holds for a stable crystal. The g values cited in Table 1 were around 0.026 and insensitive to the addition of TG gels, whereas g increased by the addition of SVN gels. These behaviors of g values are consistent to those of rigidities, i.e., distortion of crystal structures is more effective by the addition of SVN gels.

Table 1 Elastic moduli of thermo-sensitive crystals of CS82 spheres with TG and SVN gels at 25 °C

w (g/ml)	N_p+N_g	G (Pa)	g
TG gels added			
0	5.59×10^{13}	260	0.030
0.0001	5.59×10^{13}	250	0.030
0.0003	5.59×10^{13}	280	0.029
0.001	5.60×10^{13}	250	0.030
0.0025	5.61×10^{13}	280	0.029
0.003	5.61×10^{13}	267	0.029
0.0042	5.62×10^{13}	260	0.030
SVN gels added			
0	5.59×10^{13}	270	0.029
0.0001	5.59×10^{13}	260	0.030
0.0003	5.59×10^{13}	235	0.031
0.001	5.59×10^{13}	231	0.032
0.0025	5.59×10^{13}	253	0.030
0.003	5.59×10^{13}	199	0.034
0.0042	5.59×10^{13}	200	0.034
0.0083	5.59×10^{13}	135	0.041
0.01	5.59×10^{13}	96	0.049

Conclusion

Thermo-sensitive colloidal crystals were prepared simply by mixing silica and thermo-sensitive gel spheres. The lattice constants *increased* transitionally by the addition of larger gels than silica spheres (TG and SVN in this work), whereas the lattice constants *decreased* by the addition of smaller gels (KG in a previous work). The segregation effect of the gels from the crystal lattices is highly plausible for the former systems in this work.

Acknowledgments The Ministry of Education, Science, Sports and Culture is thanked for the grants-in-aids for Scientific Research on Priority Area (A) (11167241), Scientific Research (B) (11450367 and 18350057) and Germinant Research (17655046). Catalyst and Chemicals Co. (Tokyo) is appreciated for their gift of colloidal silica spheres.

References

1. Luck W, Klier M, Wesslau H (1963) Ber Bunsenges Phys Chem 67:85
2. Ottewill RH, Shaw JN (1966) Discuss Faraday Soc 42:154
3. Hiltner PA, Krieger IM (1969) J Phys Chem 73:2386
4. Kose A, Ozaki M, Takano K, Kobayashi Y, Hachisu S (1973) J Colloid Interface Sci 44:330
5. Clark NA, Hurd AJ, Ackerson BJ (1979) Nature 281:57
6. Pieranski P (1983) Contemporary Physics 24:25
7. Vanderhoff W, van de Hul HJ, Tausk RJM, Overbeek JThG (1970) Clean surfaces: their preparation and characterization for interfacial studies. Dekker, New York, 15
8. Williams R, Crandall RS, Wojtowicz PJ (1976) Phys Rev Lett 37:348
9. Mitaku S, Ohtsuki T, Enari K, Kishimoto A, Okano K (1978) Jpn J Appl Phys 17:305
10. Lindsay HM, Chaikin PM (1982) J Chem Phys 76:3774
11. Aastuen DJW, Clark NA, Cotter LK, Ackerson BJ (1986) Phys Rev Lett 57:1733
12. Okubo T (1988) Acc Chem Res 21:281
13. Lowen H, Palberg T, Simon R (1993) Phys Rev Lett 70:1557
14. Stevens MJ, Falk ML, Robbins MO (1996) J Chem Phys 104:5209

15. Pusey PN, van Megen W (1986) Nature 320:340
16. Russel WB, Saville DA, Schowalter WR (1989) Colloidal dispersions. Cambridge University Press, Cambridge
17. Sood AK (1991) Solid State Phys 45:2
18. Okubo T, Kimura K, Kimura H (2002) Colloid Polym Sci 280:1001
19. Okubo T (2005) Structural colors in biological systems. Principles and applications. Kinoshita S, Yoshioka S (eds) Osaka University Press, Osaka, p 267
20. Brock SL, Schnabria M, Suib SL, Urban V, Thiagarajan P, Potter DI (1999) J Phys Chem 103:7416
21. Jiang P, Cizeron J, Bertone JF, Colvin VL (1999) J Am Chem Soc 121:7957
22. Dimitrov AS, Miwa T, Nagayama KA (1999) Langmuir 15:5257
23. Nikoobakht B, Wang ZL, El-Sayed MA (2000) J Phys Chem B 104:8635
24. Okubo T, Okuda S, Kimura H (2002) Colloid Polym Sci 280:454
25. Okubo T, Kimura K, Kimura H (2002) Colloid Polym Sci 280:1001
26. Okubo T, Yamada T, Kimura K, Tsuchida A (2005) Colloid Polym Sci 283:1007
27. Okubo T (2006) Colloid Polym Sci 284:1191
28. Okubo T, Kimura H, Hase H, Yamaguchi K, Taniguchi T, Nagai K (2004) Colloid Polym Sci 282:250
29. Okubo T, Kimura H, Hase H, Lovell PA, Erington N, Thong P (2005) Colloid Polym Sci 283:393
30. Shibata K, Kimura H, Tsuchida A, Okubo T, Sato S, Yoshinaga K (2006) Colloid Polym Sci 284:372
31. Murray MJ, Snoedon MJ (1995) Adv Colloid Interface Sci 54:73
32. Pelton R, Wu X, Mc Phee W, Tam KC (1995) Colloidal polymer particles. Goodwin JW, Buscall R (eds) Academic, p 81
33. Kawaguchi H (1996) Biomedical functions and biotechnology of natural and artificial polymers. Yalpani M (ed) ATL Press, p 157
34. Kawaguchi H (1998) Microbeads, microcapsules and liposomes. Arshaby R (ed) STN Books, London, p 233
35. Pelton R (2000) Adv Colloid Interface Sci 85:1
36. Xia Y, Cates B, Yin Y, Lu Y (2000) Adv Mater 12:693
37. Xia Y (2001) Adv Mater 13:369
38. Okubo T, Hase H, Kimura H, Kokufuta E (2002) Langmuir 18:6783
39. Tauer K, Khrenov V (2002) Macromol Symp 179:27
40. Tsuji S, Kawaguchi H (2004) Langmuir 20:2449
41. Dhont JKG, Smits C, Lekkerkerker HNW (1992) J Colloid Interface Sci 152:386
42. Okubo T, Ishiki H (2000) J Colloid Interface Sci 228:151
43. Crandall RS, Williams R (1997) Science 198:293
44. Mitaku S, Ohtsuki T, Kishimoto A, Okano K (1980) Biophys Chem 11:411